Potentiation of the Cardiac L-Type Ca^{2+} Channel (α_{1C}) by Dihydropyridine Agonist and Strong Depolarization Occur via Distinct Mechanisms

Christina M. Wilkens,[1] Manfred Grabner,[2] and Kurt G. Beam[1]

[1]Department of Anatomy and Neurobiology, College of Veterinary Medicine and Biomedical Sciences, Colorado State University, Fort Collins, CO 80523

[2]Department of Biochemical Pharmacology, University of Innsbruck, A-6020 Innsbruck, Austria

ABSTRACT A defining property of L-type Ca^{2+} channels is their potentiation by both 1,4-dihydropyridine agonists and strong depolarization. In contrast, non–L-type channels are potentiated by neither agonist nor depolarization, suggesting that these two processes may by linked. In this study, we have tested whether the mechanisms of agonist- and depolarization-induced potentiation in the cardiac L-type channel (α_{1C}) are linked. We found that the mutant L-type channel GFP-α_{1C}(TQ→YM), bearing the mutations T1066Y and Q1070M, was able to undergo depolarization-induced potentiation but not potentiation by agonist. Conversely, the chimeric channel GFP-CACC was potentiated by agonist but not by strong depolarization. These data indicate that the mechanisms of agonist- and depolarization-induced potentiation of α_{1C} are distinct. Since neither GFP-CACC nor GFP-CCAA was potentiated significantly by depolarization, no single repeat of α_{1C} appears to be responsible for depolarization-induced potentiation. Surprisingly, GFP-CACC displayed a low estimated open probability similar to that of the α_{1C}, but could not support depolarization-induced potentiation, demonstrating that a relatively low open probability alone is not sufficient for depolarization-induced potentiation to occur. Thus, depolarization-induced potentiation may be a global channel property requiring participation from all four homologous repeats.

KEY WORDS: ion channel modulation • facilitation • muscle

INTRODUCTION

Voltage-gated Ca^{2+} channels respond to membrane depolarization by allowing Ca^{2+} into the cell, and, thus, mediate a variety of cellular responses in neurons and muscle, including transmitter release, neurite outgrowth, altered gene expression, exocytosis, and muscle contraction (Reuter, 1983; Hoshi and Smith, 1987; Tsien et al., 1988; Tanabe et al., 1993). Thus, modification of Ca^{2+} influx provides an important mechanism for the regulation of many downstream Ca^{2+}-dependent responses. One source of modification is potentiation, whereby a channel is stabilized in the open state, and intracellular Ca^{2+} levels are increased as a result.

L-type Ca^{2+} channels show a shift in gating mode in response to either strong depolarization or 1,4-dihydropyridine (DHP)* agonist. After strong depolarization, the channel enters a state of higher open probability (P_o) and long open times that can be detected by a number of different pulse paradigms. For example, after a strong, conditioning depolarization (e.g., +120 mV) followed by a 50–150-ms return to the holding potential, a subsequent, moderate depolarization elicits a Ca^{2+} channel current that is about twofold larger than that measured without the conditioning depolarization (Bourinet et al., 1994; Cens et al., 1996, 1998). This effect, which implies an alteration of gating that persists after channel closing, will be designated "depolarization-induced facilitation." Both L- and non–L-type channels are also able to undergo another form of prepulse facilitation ("Ca^{2+}/CAM-dependent facilitation"; Lee et al., 2000; Zühlke et al., 2000; DeMaria et al., 2001), which differs from depolarization-induced facilitation in that it has a bell-shaped dependence on the prepulse potential that arises from a primary dependence upon Ca^{2+} entry. Ca^{2+}/CAM-dependent facilitation appears to depend specifically (Lee et al., 2000) upon the β_{2a} subunit, and does not occur in cells expressing β_1, the isoform present in the dysgenic myotubes used in our study. Unlike Ca^{2+}/CAM-dependent facilitation, depolarization-induced facilitation may be related to another form of altered gating observed when a strong depolarization is followed immediately by repolarization to an intermediate potential (Hoshi and Smith, 1987; Pietrobon and Hess, 1990; Kleppisch et al., 1994). This phenomenon, referred to here as de-

Address correspondence to Kurt Beam, Department of Anatomy and Neurobiology, College of Veterinary Medicine and Biomedical Sciences, Colorado State University, Fort Collins, CO 80523. Fax: (970) 491-7907; E-mail: kbeam@lamar.colostate.edu

*Abbreviations used in this paper: DHP, 1,4-dihydropyridine; GFP, green fluorescent protein; nt, nucleotide; P_o, open probability.

polarization-induced potentiation, results in a mode of gating characterized at the single-channel level by high P_o and long open times, which is also referred to as "mode 2" gating (Pietrobon and Hess, 1990). As an indication of depolarization-induced entry into mode 2, we have measured whole-cell tail currents upon repolarization to −50 mV immediately after a strong, conditioning depolarization. With this protocol, high P_o and long open times are reflected by an increased tail-current amplitude and slower rate of tail-current decay, respectively. Mode 2 gating of L-type channels is also promoted by DHP agonists (Hess et al., 1984; Nowycky et al., 1985; Hoshi and Smith, 1987). Given the similarities between agonist- and depolarization-induced potentiation, it is important to know the degree to which the two processes are related.

The cardiac L-type channel, α_{1C}, normally exhibits a low $P_o < 0.05$ (Cachelin et al., 1983; Lew et al., 1991) and can be potentiated by both strong depolarization and DHP agonists. By contrast, the neuronal non–L-type channel, α_{1A}, exhibits a high P_o of ∼0.6 (Llinas et al., 1989) and lacks both depolarization-induced facilitation (Bourinet et al., 1994), and DHP-induced potentiation (Sather et al., 1993). These observations suggest the possibility that depolarization- and agonist-induced potentiation can only occur in channels like α_{1C} that have an intrinsically low P_o.

In an attempt to determine whether potentiation of α_{1C} by DHP agonist and strong depolarization occurs via a common pathway, we have characterized wild-type and mutant α_{1C} channels and chimeric channels composed of α_{1C} and α_{1A} sequence. The channels were fused at their amino termini to green fluorescent protein (GFP), expressed in dysgenic myotubes and examined using whole-cell patch clamp. For an α_{1C} in which the agonist binding site was mutated (GFP-α_{1C}(TQ→YM)), 10 μM Bay K 8644 had no significant effect on whole-cell currents, whereas depolarization-induced potentiation remained intact. A chimeric channel containing repeat II and the I-II linker of α_{1A} sequence embedded in L-type background (GFP-CACC) could not support depolarization-induced potentiation but was potentiated by DHP agonist. Channels containing three (CACC), two (CCAA), or no (α_{1A}) repeats of L-type sequence were not potentiated significantly by depolarization, suggesting that depolarization-induced potentiation cannot be localized to any single channel repeat. Interestingly, despite having a relatively low estimated P_o comparable to that of α_{1C}, GFP-CACC was not potentiated by depolarization, indicating that depolarization-induced potentiation must not be dependent solely on a low P_o. Our results demonstrate that the mechanisms of DHP agonist- and depolarization-induced potentiation of α_{1C} are distinct, and that depolarization-induced potentiation may be a global channel property requiring the participation of all four homology repeats.

MATERIALS AND METHODS

Construction of Chimeric and Mutant α_1 cDNAs

A and C denote sequence derived from α_{1A} (Mori et al., 1991) or α_{1C} (Mikami et al., 1989), respectively. An asterisk indicates a restriction site introduced by PCR. The wild-type clones GFP-α_{1C} and GFP-α_{1A} were produced by fusing the α_1 subunit of either the cardiac L-type channel (α_{1C}) or neuronal P/Q-type channel (α_{1A}) at the amino terminus to GFP as previously described (Grabner et al., 1998). The GFP tag has been shown not to alter any of the functional properties of the α_{1C} and α_{1A} subunits (Grabner et al. 1998). The clone GFP-α_{1C}(TQ→YM) was created using overlapping PCR mutagenesis (Horton et al., 1989) to replace two residues in the IIIS5 transmembrane domain of α_{1C} (Thr 1066 and Gln 1070), which were previously identified as essential components of the DHP binding site (Mitterdorfer et al., 1996; He et al., 1997), with the corresponding residues of α_{1A} (Tyr 1393 and Met 1397). In brief, the SalI*-FspI fragment of α_{1C} (nt −12C–5054C) was subcloned into the SalI and SmaI sites of the pSP72 (Promega) polylinker. Overlapping PCR using GFP-α_{1C} as the template yielded an 816-bp amplification product (nt 2638C–3453C) carrying the point mutations, which was then cut with AflII (nt 2689) and AspI (nt 3385) and ligated into the AflII-AspI restriction sites of the pSP72 subclone. Finally, the SalI*-EcoRV fragment (nt −12C–4348C) of the subclone was ligated into GFP-α_{1C} at the corresponding restriction sites to yield the clone GFP-α_{1C}(TQ→YM). The α_{1C}/α_{1A} chimera GFP-CACC consisted of repeat II and the I-II linker of α_{1A} contained an α_{1C} background (amino acids 1–426C/352–671A/740–2171C). To produce GFP-CACC, the SalI*-EcoRV fragment of α_{1C} (nt −12C–4348C) was ligated into the corresponding sites of the plasmid pSP72. PCR mutagenesis was used to amplify a 980-bp product of α_{1A} sequence, containing the introduced 5′ BamHI* and 3′ EcoRI* restriction sites at nt 1039 and 2015, respectively. The amplification product was first digested with BamHI, and then partially digested with EcoRI (to avoid cutting an internal EcoRI site), and the resulting fragment was ligated into the corresponding restriction sites of the pSP72/cardiac subclone. Finally, the SalI*-EcoRV fragment from this subclone was ligated into the SalI*-EcoRV restriction sites of GFP-α_{1C}. The chimera GFP-CCAA was composed of repeats I and II (including the II-III linker) of α_{1C} and repeats III and IV of α_{1A} (amino acids 1-920C/1244-2424A). To create GFP-CCAA, the HindIII*-PvuII fragment (nt 3730A–4216A) of chimera AL2 (Grabner et al., 1996) was coligated with the PvuII-BglII fragment of α_{1A} (nt 4216A–5891A) into the corresponding restriction sites of the plasmid pSP72. Subsequently, the XhoI-HindIII* fragment (nt 1395A–2758C) of clone AL5 (Grabner et al., 1996) was ligated into the corresponding restriction sites of the subclone. The entire XhoI-BglII insert (nt 1395A–5891A) of the final subclone was ligated into the corresponding restriction sites of GFP-α_{1A} to produce the intermediate clone GFP-ALC. The SalI*-AvrII fragment (nt −12C–759C) of GFP-α_{1C} was coligated with the AvrII-AocI fragment (nt 759C–1752A) of AL5 into the SalI-AocI (5′ polylinker-1752A) restriction sites of GFP-ALC, yielding the subclone GFP-C/3A. Finally, the ClaI-AflII fragment (nt 256C–2689C) of α_{1C} was ligated into the corresponding restriction sites of subclone GFP-C/3A to yield the final chimera GFP-CCAA. The integrity of all channel constructs was confirmed using automated sequence analysis (Macromolecular Resources).

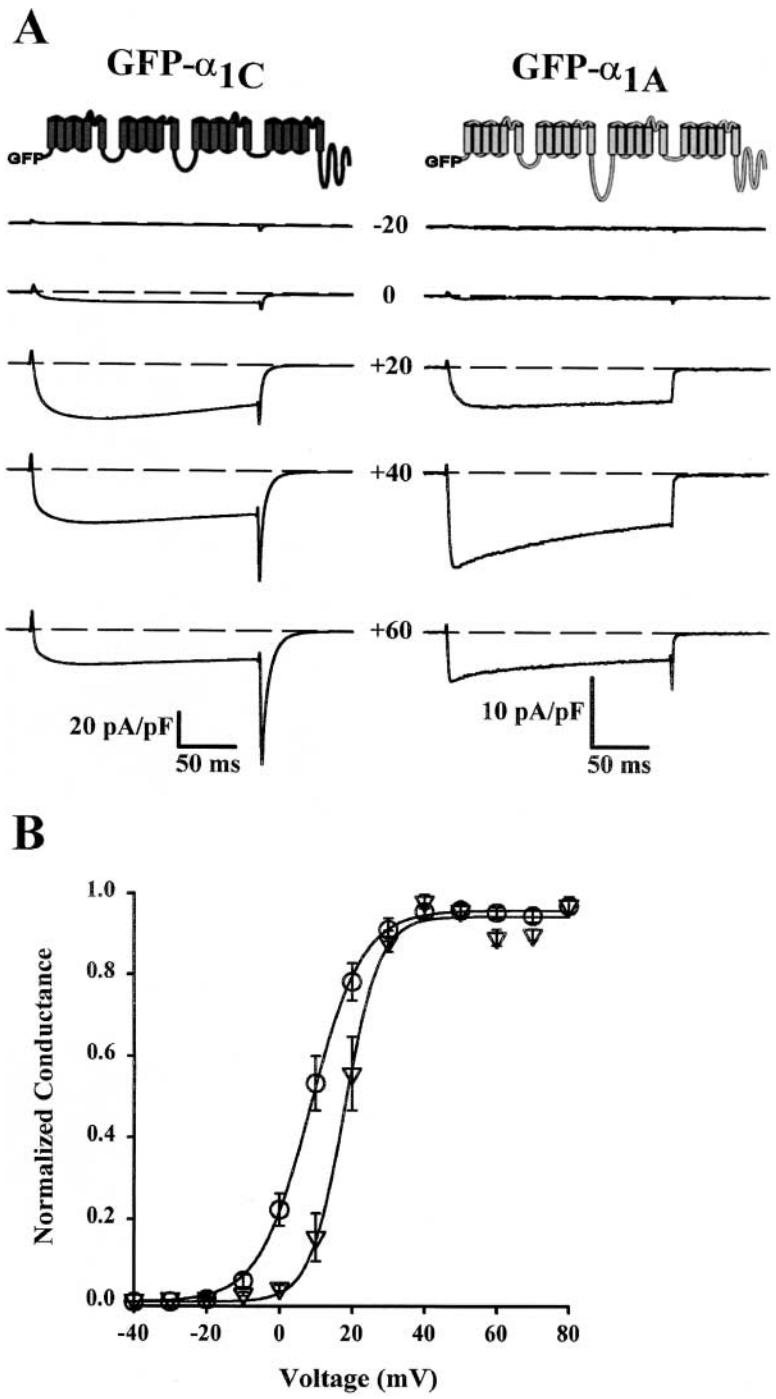

FIGURE 1. Activation of currents produced by GFP-α_{1C} or GFP-α_{1A} expressed in dysgenic myotubes. (A) Representative Ca^{2+} currents elicited by 200-ms depolarizing steps to the indicated test potentials from a holding potential of −80 mV, followed by repolarization to −50 mV. Putative membrane topology for each GFP-tagged channel construct is indicated, where dark gray and light gray represent α_{1C} and α_{1A} sequence, respectively. (B) Average (± SEM) conductance versus voltage relationships for GFP-α_{1C} (circles; $n = 9$) and GFP-α_{1A} (inverted triangles; $n = 10$). The smooth curves represent best fits of the expression $1/\{1 + \exp[-(V - V_{1/2})/k_G]\}$, which yielded the following values: for GFP-α_{1C}, $V_{1/2} = 8$ mV, $k_G = 7.3$ mV; and for GFP-α_{1A}, $V_{1/2} = 19$ mV, $k_G = 5.1$ mV.

Expression and Electrophysiological Analysis of Channels in Dysgenic Myotubes

1 wk after plating, primary cultures of mouse dysgenic myotubes (Adams and Beam, 1989), which lack an endogenous α_{1S} subunit (Knudson et al., 1989), were microinjected in single nuclei with cDNAs (200–600 ng/μl) encoding GFP-tagged α_1 subunits. 36–52 h after injection, expressing myotubes were identified by green fluorescence and used for electrophysiology. Macroscopic Ca^{2+} currents were measured using the whole-cell patch-clamp method (Hamill et al., 1981). Whole-cell patch pipettes of borosilicate glass had resistances of 1.5–2.0 MΩ when filled with an internal solution containing 140 mM cesium aspartate, 10 mM Cs_2EGTA, 5 mM $MgCl_2$, and 10 mM HEPES, pH 7.4 with CsOH. The external bath solution contained 10 mM $CaCl_2$, 145 mM TEA-Cl, and 10 mM HEPES, pH 7.4 with TEA-OH, plus 3 μM tetrodotoxin. Test currents were obtained by stepping from a holding potential of −80 to −30 mV for 1 s (to inactivate endogenous T-type Ca^{2+} current; Adams et al., 1990), to −50 mV for 30–50 ms, to the test potential for 200 ms, to −50 mV for 125 ms, and back to −80 mV. Test currents were corrected for linear components of leak and capacitative currents by digitally scaling and subtracting the average of 10 preceding control currents elicited by hyperpolarizing steps (20–40 mV in amplitude) applied from

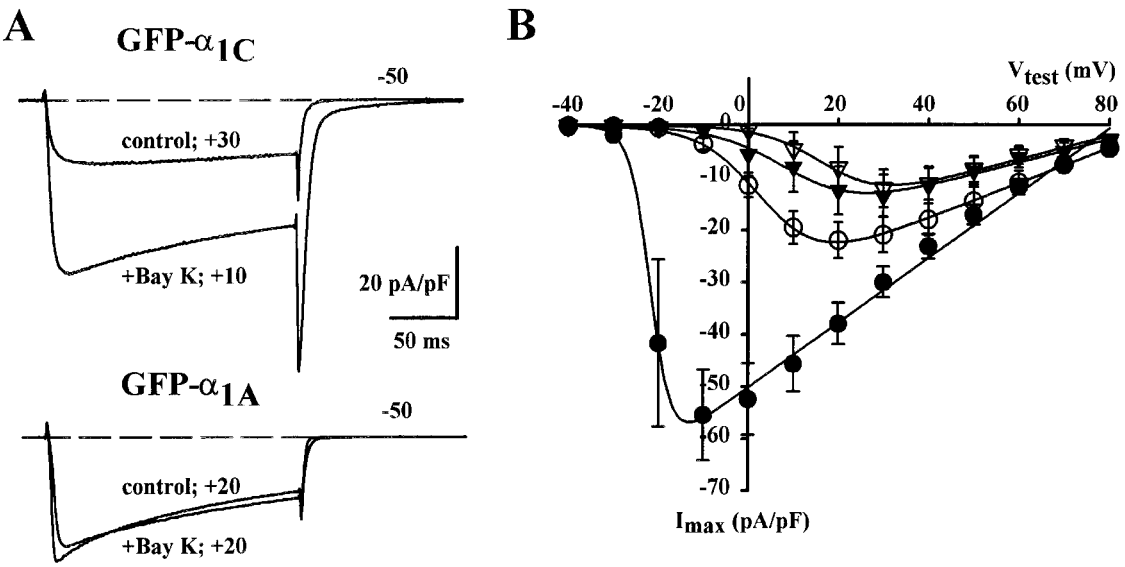

FIGURE 2. Dihydropyridine agonist potentiates GFP-α_{1C} but not GFP-α_{1A}. (A) Peak Ca^{2+} currents from GFP-α_{1C} (top) or GFP-α_{1A} (bottom) elicited by 200-ms depolarizations to the indicated test potentials in the absence (control) and presence (+Bay K) of 10 μM Bay K 8644. (B) Average current versus voltage relationships for GFP-α_{1C} (circles; $n = 5$) and GFP-α_{1A} (inverted triangles; $n = 7$) in the absence (open symbols) or presence (closed symbols) of 10 μM Bay K 8644. The smooth curves represent best fits of Eq. 1 to the average data resulting in the values (control/+Bay K): for GFP-α_{1C}, G_{max} = 337 nS/nF/620 nS/nF, $V_{1/2}$ = 4 mV/−22 mV, V_{rev} = 93 mV/81 mV, k_G = 7 mV/2 mV; and for GFP-α_{1A}, G_{max} = 228 nS/nF/225 nS/nF, $V_{1/2}$ = 18 mV/11 mV, V_{rev} = 88 mV/91 mV, k_G = 7 mV/8 mV.

the holding potential. Data were included only for cells in which the maximum voltage error (calculated by the product of peak inward current and compensated series resistance) was ≤10 mV. Except for tail currents, data were sampled at 1 kHz. Tail currents, elicited by repolarizing to −50 mV for 125 ms, were recorded with fast sampling (10 kHz). Tail-current amplitude (I_{tail}) was measured 0.5 ms after the onset of the repolarization from the test pulse to −50 mV. The rate of tail-current decay (τ_{deact}) was measured by fitting tail currents with a single exponential function. Maximal Ca^{2+} conductance (G_{max}) and half-maximal activation potential ($V_{1/2}$) were calculated by fitting peak inward current values with the equation:

$$I = G_{max} \cdot (V - V_{rev})/(\{1 + \exp[-(V - V_{1/2})/k_G]\},) \qquad (1)$$

where I is the peak inward Ca^{2+} current measured at the test potential (V), V_{rev} is the reversal potential, and k_G is a slope factor. The values of G_{max} and V_{rev} were used to calculate normalized conductance as a function of voltage (see Figs. 1 A and 4 C) according to the equation: $G(V) = I/[G_{max} \cdot (V - V_{rev})]$.

Maximum immobilization-resistant charge movement (Q_{max}) was measured, after the addition of 0.5 mM Cd^{2+} and 0.1 mM La^{3+} to the bath, by integration of Q_{on} for a 15-ms test pulse (exponentially rounded with a time constant of 100 μs) to +40 mV. Maximum channel P_o was calculated from the average, measured values of $\overline{G_{max}}$ and $\overline{Q_{max}}$ according to the equation:

$$P_o = (q \cdot \overline{G_{max}}' \cdot F)/(\gamma \cdot \overline{Q_{max}}' \cdot A), \qquad (2)$$

where $\overline{Q_{max}}' = \overline{Q_{max}}$ - average dysgenic charge (2.5 nC/μF; Adams et al., 1990), γ is the single-channel conductance in 10 mM Ca^{2+}, assumed to be 4 pS for α_{1A} (Adams et al., 1994), 5.8 pS for α_{1C} (Gollasch et al., 1992), or an average of the two (4.9 pS) for chimeras CACC and CCAA, q is the assumed single-channel gating charge (9 e^-; Noceti et al., 1996), F is Faraday's constant (96,487 C/mol) and A is Avogadro's number (6.023×10^{23} e^-/mol).

Several different measures were used to quantify potentiation. For the DHP agonist (±)Bay K 8644, one measure was the ratio $I_{max}^{Bay\,K}/I_{max}^{control}$, where the numerator and denominator represent the peak currents elicited by depolarizing test pulses in the presence or absence of drug, respectively. $I_{max}^{control}$ was usually elicited by a V_{test} of approximately +20–30 mV, and $I_{max}^{Bay\,K}$ for a V_{test} 20–30 mV more hyperpolarized. Agonist-induced potentiation was also measured by means of the ratios $I_{tail}^{Bay\,K}/I_{tail}^{control}$ and $\tau_{deact}^{Bay\,K}/\tau_{deact}^{control}$, where the tail current was produced by repolarizing to −50 mV from a V_{test} of +40 mV. Depolarization-induced potentiation was quantified by the ratios $I_{tail}^{+90}/I_{tail}^{+40}$ and $\tau_{deact}^{+90}/\tau_{deact}^{+40}$, where the numerator and denominator were determined from tail currents produced by repolarization to −50 mV after a V_{test} of +90–110 mV or +40 mV, respectively.

Statistical Analysis

Statistical significance was assessed using one-way analysis of variance (ANOVA) and SAS software (version 8). All data are presented as mean ± SEM.

RESULTS

α_{1C} Is Potentiated by DHP Agonist and Strong Depolarization while α_{1A} Is Potentiated by Neither

Fig. 1 A illustrates representative whole-cell Ca^{2+} currents elicited by depolarizing dysgenic myotubes expressing either GFP-α_{1C} or GFP-α_{1A} to the indicated potentials, followed by repolarization to −50 mV. Based upon steady-state activation calculated from peak currents during the test depolarizations (Fig. 1 B), both channels were fully activated by test pulses to +40 mV

TABLE I

Parameters of DHP Agonist- and Depolarization-induced Potentiation

	GFP-α_{1C}	GFP-α_{1C}(TQ→YM)	GFP-CACC	GFP-CCAA	GFP-α_{1A}
Depolarization-induced potentiation of I_{tail}	1.9-fold ± 0.3 (8)	2.5-fold ± 0.3 (11)	1.3-fold ± 0.1 (8)	1.1-fold ± 0.3 (7)	0.9-fold ± 0.1 (8)
Depolarization-induced potentiation of τ_{deact}	2.6-fold ± 0.8 (5)	2.7-fold ± 0.3 (8)	1.2-fold ± 0.1 (8)	1.0-fold ± 0.1 (7)	0.9-fold ± 0.1 (6)
Bay K-induced potentiation of I_{max}	2.7-fold ± 0.2 (5)	0.9-fold ± 0.1 (7)	3.4-fold ± 0.9 (5)	1.0-fold ± 0.1 (9)	1.1-fold ± 0.1 (7)
Bay K-induced activation shift ($V_{1/2}$; mV)	−24.9 ± 4.1 (5)	−3.3 ± 4.2 (6)	−15.7 ± 5.4 (5)	−3.0 ± 0.9 (9)	−3.9 ± 1.2 (6)
Bay K-induced potentiation of I_{tail}	3.3-fold ± 0.6 (5)	0.9-fold ± 0.1 (7)	6.2-fold ± 3.7 (5)	1.3-fold ± 0.4 (9)	1.2-fold ± 0.1 (6)
Bay K-induced potentiation of τ_{deact}	2.9-fold ± 0.5 (5)	1.2-fold ± 0.1 (7)	3.0-fold ± 0.9 (5)	1.1-fold ± 0.1 (9)	1.2-fold ± 0.1 (6)

I_{tail} and τ_{deact} were determined as the amplitude (0.5 ms after repolarization) and time constant of decay (determined by fit of a single exponential) of tail currents produced by repolarization to −50 mV. Depolarization-induced potentiation was quantified as the ratios ($(I_{tail}^{+90}/I_{tail}^{+40})$) or ($\tau_{deact}^{+90}/\tau_{deact}^{+40}$), where the superscripts indicate the test potential before repolarization. The effect of 10 μM Bay K 8644 was quantified in terms of four parameters: the ratio of maximum currents ($I_{max}^{Bay\,K}/I_{max}^{control}$); the average shift in the voltage for half-maximal activation ($V_{1/2}^{Bay\,K} - V_{1/2}^{control}$); and the ratio of the values of I_{tail} ($I_{tail}^{Bay\,K}/I_{tail}^{control}$) and τ_{deact} ($\tau_{deact}^{Bay\,K}/\tau_{deact}^{control}$) after a test to +40 mV. All data are presented as mean ± SEM, with the numbers in parentheses indicating the number of cells tested.

and above. Consistent with this, the tail currents for GFP-α_{1A} had a similar amplitude and time course after the depolarizations to either +40 or +60 mV (Fig. 1 A). However, for GFP-α_{1C}, the tail current after the +60-mV depolarization was larger and decayed more slowly than the tail after the +40-mV step. This behavior is an indication that strong depolarization caused α_{1C} channels to enter a mode of gating having longer open times and increased P_o.

Fig. 2 compares currents produced by GFP-α_{1C} and GFP-α_{1A} before and after exposure to 10 μM Bay K 8644. For GFP-α_{1A}, application of Bay K 8644 had little effect on either the current elicited by a test depolarization to +20 mV or on the tail current after repolarization (Fig. 2 A). Likewise, the average, peak current versus voltage relationship for GFP-α_{1A} was not significantly ($P > 0.1$) affected by the agonist (Fig. 2 B). By contrast, Bay K 8644 caused a hyperpolarizing shift in the test potential evoking maximum inward current for GFP-α_{1C}, together with a substantial increase in the magnitude of this current. In addition to affecting the peak current, Bay K 8644 also caused an approximately threefold increase in tail-current amplitude (I_{tail}) and in the time constant of tail-current deactivation (τ_{deact}) for GFP-α_{1C} (Fig. 2 A and Table I). Overall, the effects of Bay K 8644 on GFP-α_{1C} tail currents qualitatively resemble those of strong depolarization (compare Figs. 1 A and 2 A).

Fig. 3 illustrates a more detailed characterization of tail currents in cells expressing GFP-α_{1C} or GFP-α_{1A}. Fig. 3 A shows the standard protocol for quantifying depolarization-induced potentiation, which was determined as the ratio of either I_{tail} or τ_{deact} for a tail current after a V_{test} of +90 mV, to the corresponding values for a tail current after a V_{test} of +40 mV. By both measures, GFP-α_{1C} showed substantial depolarization-induced potentiation, whereas GFP-α_{1A} did not (Fig. 3 A and Table I). Fig. 3 B illustrates the dependence of I_{tail} on prior test potentials ranging from −40 to +80 mV. For GFP-α_{1A}, I_{tail} reached a maximum after a V_{test} of +30 mV, in good agreement with the conductance versus voltage curve calculated from peak currents (Fig. 1 B). For still stronger depolarizations, I_{tail} became smaller for GFP-α_{1A}, as expected for a channel undergoing voltage-dependent inactivation that becomes faster with stronger depolarization. In contrast to GFP-α_{1A}, I_{tail} for GFP-α_{1C} increased monotonically over the entire range of test potentials. This monotonic increase differs from the saturating conductance versus voltage relationship (Fig. 1 B) and is consistent with entry into a potentiated state having high P_o. This monotonic voltage dependence also suggests that depolarization-induced potentiation is not dependent upon Ca^{2+} entry during the prepulse. The application of 10 μM Bay K 8644 caused a still further increase in P_o, which is indicated by a substantial increase in I_{tail} for GFP-α_{1C} at any given test potential (Fig. 3 B). In the presence of agonist, I_{tail} was still increased by stronger test depolarizations, up to at least +70 mV. Table I summarizes the effects of DHP agonist and strong depolarization on tail currents for GFP-α_{1C} and GFP-α_{1A}.

Mutation of T1066 and Q1070 of α_{1C} Eliminates Agonist- but Not Depolarization-induced Potentiation

The observation that GFP-α_{1C} is potentiated by both agonist and strong depolarization, whereas GFP-α_{1A} is potentiated by neither, raises the possibility that agonist- and depolarization-induced potentiation are linked. As one test of this hypothesis, we created GFP-

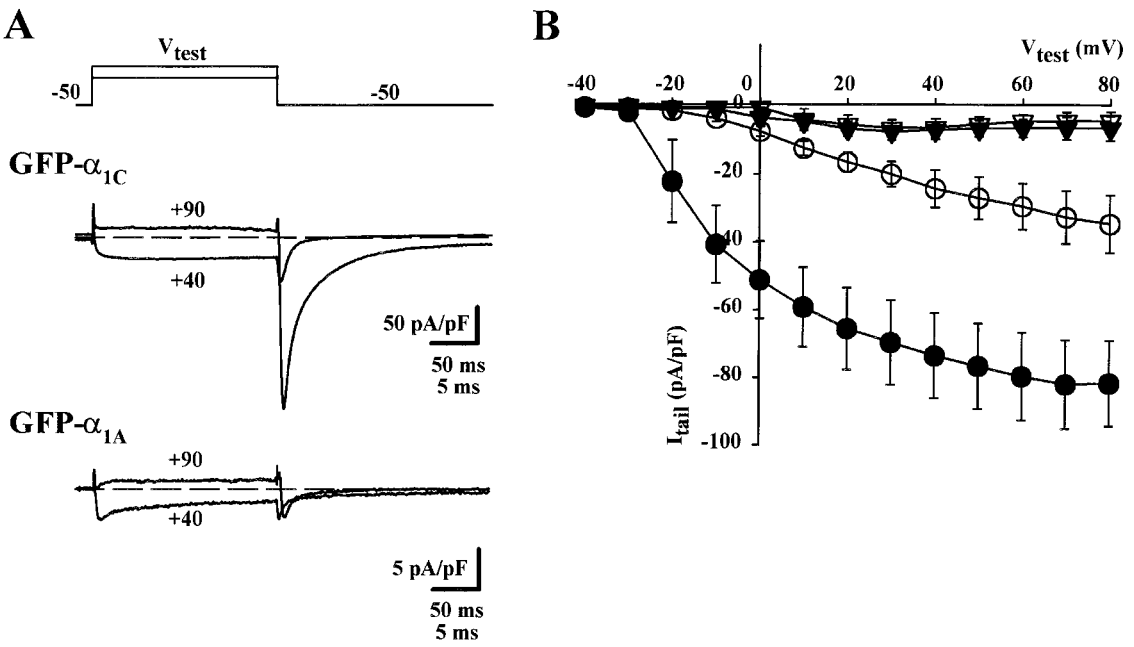

FIGURE 3. Depolarization-induced potentiation of GFP-α_{1C} but not of GFP-α_{1A}. (A) Tail currents were elicited by depolarization from the holding potential (−80 mV) to −30 mV for 1 s (to inactivate endogenous T-type current; Adams et al., 1990), a 30–50-ms repolarization to −50 mV, a 200-ms test depolarization (V_{test}) to varying potentials, followed by repolarization to −50 mV. Whole-cell currents are shown for GFP-α_{1C} (top) and GFP-α_{1A} (bottom) for test depolarizations of +40 and +90 mV. Note that for GFP-α_{1C}, the tail current after the V_{test} of +90 mV was larger and decayed more slowly than that after the V_{test} of +40 mV, whereas the tail currents for GFP-α_{1A} differed little for a V_{test} of +40 or +90 mV. The 50-ms time calibration applies to the currents during the test depolarization and the 5-ms calibration to the tail currents at −50 mV. (B) Relationship of tail-current amplitude (I_{tail}) at −50 mV to test pulse potential (V_{test}) for cells expressing GFP-α_{1C} (circles; $n = 5$) or GFP-α_{1A} (inverted triangles; $n = 7$) in the absence (open symbols) or presence (closed symbols) of 10 μM Bay K 8644. The amplitude of the tail currents for GFP-α_{1C} grew larger with increasing V_{test} over the entire range of potentials examined, whereas those for GFP-α_{1A} appeared to saturate with peak current.

α_{1C}(TQ→YM), in which two residues of IIIS5 that are critical for the DHP sensitivity of α_{1C} (Mitterdorfer et al., 1996; He et al., 1997) were converted to the corresponding residues of α_{1A}. Currents produced by GFP-α_{1C}(TQ→YM) were not affected by the addition of 10 μM Bay K 8644 (Fig. 4 A), whereas depolarization-induced potentiation was intact (Fig. 4 B). In particular, tail currents were larger and decayed more slowly after a V_{test} of +90 mV compared with a V_{test} of +40 mV (Fig. 4 B, top) and the tail-current amplitude increased monotonically as a function of test potential (Fig. 4 B, bottom). On average, GFP-α_{1C}(TQ→YM) was quantitatively similar to GFP-α_{1C} with respect to depolarization-induced potentiation, but was indistinguishable from GFP-α_{1A} in the lack of agonist-induced potentiation (Table I). Interestingly, mutation of T1066 and Q1070 in the IIIS5 transmembrane segment of α_{1C} resulted in a decreased steepness, and positive shift, of the steady-state activation curve in comparison to GFP-α_{1C} (Fig. 4 C), indicating that these residues can affect activation gating. Taken together, the data of Fig. 4 demonstrate that depolarization-induced potentiation still occurs in a mutant α_{1C} lacking a response to DHP agonist.

Agonist-induced Potentiation Persists in the Absence of Depolarization-induced Potentiation

In an attempt to determine whether a single repeat of α_{1C} is sufficient to allow depolarization-induced potentiation, we constructed the chimeras GFP-CACC and GFP-CCAA and tested them for agonist- and depolarization-induced potentiation (Fig. 5). GFP-CACC consists of repeat II and the I-II linker of α_{1A} in an otherwise α_{1C} background (Fig. 5, A and C), and thus contains an intact DHP agonist binding site (Grabner et al., 1996; Hockerman et al., 1997; Ito et al., 1997; Sinnegger et al., 1997). As shown in Fig. 5 A, 10 μM Bay K 8644 potentiated maximum inward current in cells expressing GFP-CACC and caused a leftward shift in the peak current versus voltage relationship. Quantitatively, both effects were similar to those of 10 μM Bay K 8644 on GFP-α_{1C} (Table I). However, this chimera failed to show the large depolarization-induced potentiation characteristic of either GFP-α_{1C} or GFP-α_{1C}(TQ→YM) (Table I; also, compare Fig. 5 C with Figs. 3 B and 4 B). Thus agonist-induced potentiation can be present in a channel construct that lacks significant depolarization-induced potentiation. The chimera GFP-CCAA (Fig. 5, B and D) consists of the first two repeats and the II-III

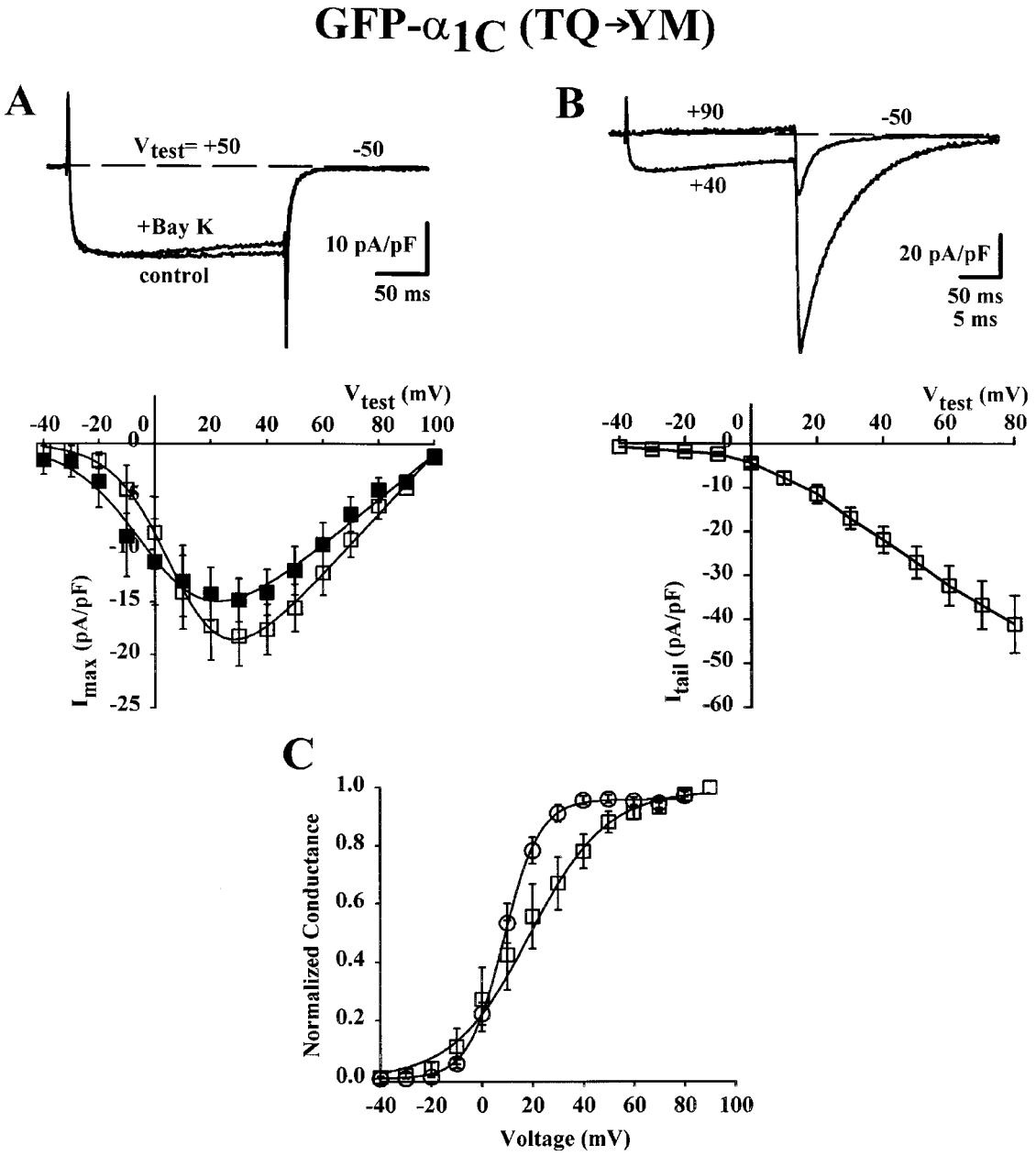

FIGURE 4. Mutation of the agonist binding site of GFP-α_{1C} abolishes potentiation by agonist (A) but not by depolarization (B). (A, top) Whole-cell currents from a myotube expressing GFP-α_{1C}(TQ→YM) in the absence (control) or presence (+Bay K) of 10 μM Bay K 8644. (A, bottom) Average peak current versus voltage relationship for GFP-α_{1C}(TQ→YM) in the absence (open squares; $n = 7$) or presence (closed squares; $n = 7$) of 10 μM Bay K 8644. The smooth curves represent best fits of the data with Eq. 1, yielding the values (control/+Bay K): G_{max} = 287 nS/nF/218 nS/nF, $V_{1/2}$ = 9 mV/1 mV, V_{rev} = 103 mV/104 mV, k_G = 10 mV/13 mV. (B, top) Whole-cell currents for GFP-α_{1C}(TQ→YM) measured for test pulses to +40 or +90 mV, followed by repolarization to −50 mV; for clarity, the tail currents at −50 mV are shown on a faster time scale (5-ms calibration bar). (B, bottom) Tail-current amplitudes at −50 mV as a function of a prior test potential for GFP-α_{1C}(TQ→YM) (open squares; $n = 11$). (C) Conductance versus voltage relationships for GFP-α_{1C} (circles; $n = 9$) and GFP-α_{1C}(TQ→YM) (squares; $n = 10$). The smooth lines represent best fits of the data with the expression: $1/\{1 + \exp[-(V - V_{1/2})/k_G]\}$, yielding the following values: for GFP-α_{1C}, $V_{1/2}$ = 9 mV, k_G = 7 mV; and for GFP-α_{1C}(TQ→YM), $V_{1/2}$ = 20 mV, k_G = 16 mV.

linker of α_{1C} fused to repeats III and IV of α_{1A}. GFP-CCAA lacked both agonist- and depolarization-induced potentiation (Fig. 5, B and D, and Table I). Fig. 6 summarizes the effects of strong depolarization and DHP agonist on the constructs GFP-α_{1C}, GFP-α_{1C}(TQ→YM), GFP-CACC, and GFP-α_{1A}. The asterisks indicate a significant ($P < 0.05$) difference from onefold (where onefold indicates a lack of potentiation). Fig. 6 demonstrates that depolarization-induced potentiation can persist in the absence of potentiation by agonist (i.e.,

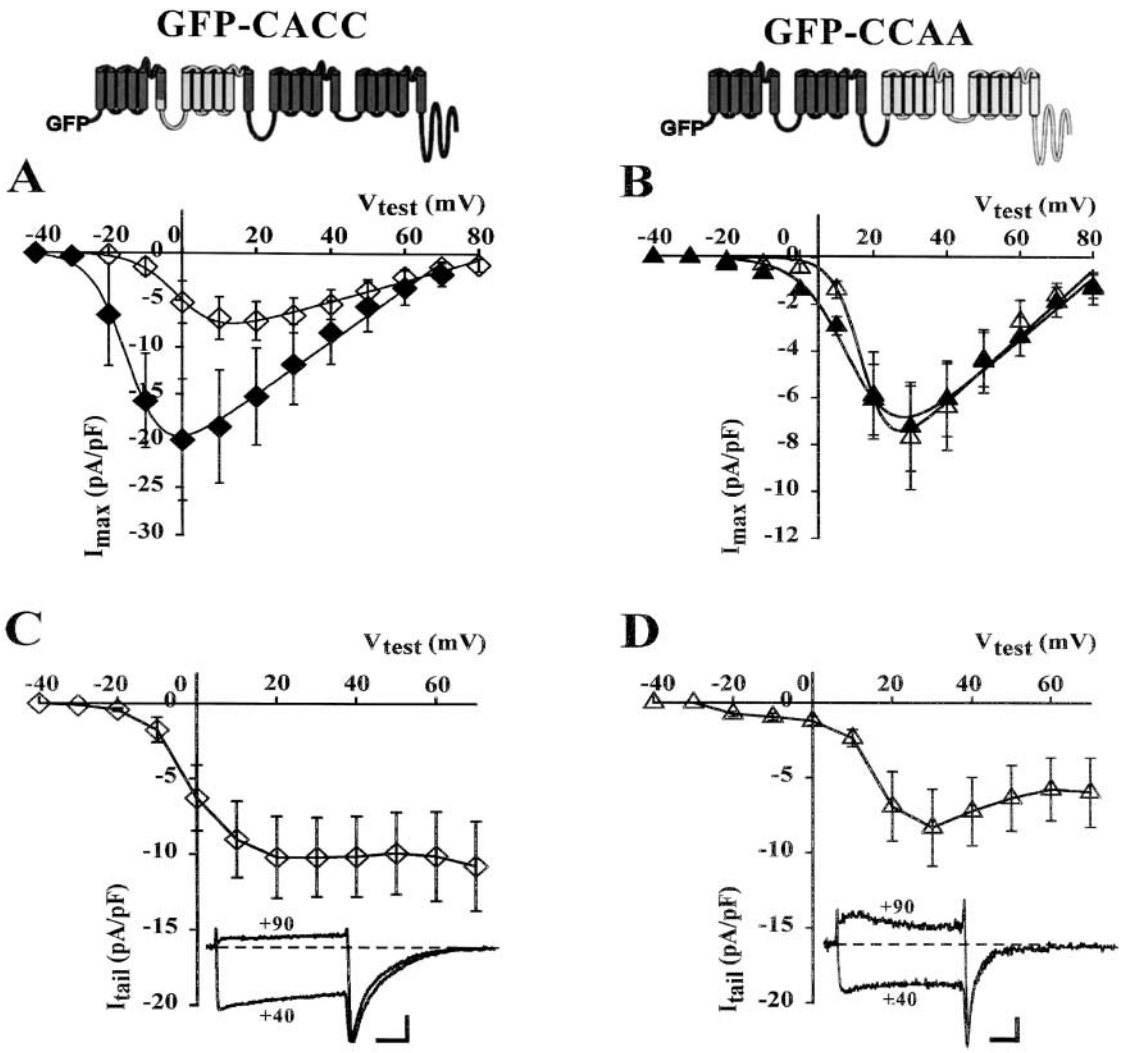

FIGURE 5. Presence or absence of potentiation by agonist or depolarization for chimeric channels. The chimeric channels GFP-CACC and GFP-CCAA are represented schematically with dark gray and light gray representing regions derived from α_{1C} and α_{1A}, respectively. (A and B) Average peak current versus voltage relationships for cells expressing GFP-CACC (diamonds; $n = 5$) or GFP-CCAA (triangles; $n = 7$), in the absence (open symbols) or presence (closed symbols) of 10 μM Bay K 8644. The smooth lines represent best fits of Eq. 1 to the average data, yielding the following values (control/+Bay K): for GFP-CACC, G_{max} = 111 nS/nF/283 nS/nF, $V_{1/2}$ = 0 mV/−14 mV, V_{rev} = 86 mV/73 mV, k_G = 6 mV/5 mV; and for GFP-CCAA, G_{max} = 142 nS/nF/133 nS/nF, $V_{1/2}$ = 17 mV/15 mV, V_{rev} = 84 mV/86 mV, k_G = 4 mV/7 mV. (C and D) Average values of tail-current amplitudes as a function of test potential for cells expressing GFP-CACC (open diamonds; $n = 8$) or GFP-CCAA (open triangles; $n = 7$). Insets illustrate superimposed currents elicited by test depolarizations to +90 or +40 mV, with the horizontal scale bars corresponding to 5 ms for the tail currents and 50 ms during the test depolarization. The vertical scale bars correspond to either 5 pA/pF (C) or 1 pA/pF (D). GFP-CACC was potentiated by agonist but not depolarization, whereas GFP-CCAA was potentiated by neither.

GFP-α_{1C}(TQ→YM)), and potentiation by agonist can occur in the absence of depolarization-induced potentiation (i.e., GFP-CACC); therefore, the two processes likely occur via distinct mechanisms.

No Single Repeat of α_{1C} Is Sufficient for Depolarization-induced Potentiation

Fig. 7 shows that in terms of both amplitude of tail currents (A) and τ_{deact} (B), the chimeras GFP-CACC and GFP-CCAA, like α_{1A}, lacked depolarization-induced potentiation. Because GFP-CACC lacked depolarization-induced potentiation, none of the three cardiac repeats contained in this construct (i.e., I, III, and IV) appears to be sufficient, individually or in concert, to mediate this process. In addition, because GFP-CCAA contains a cardiac repeat II and lacked depolarization-induced potentiation, a cardiac repeat II does not appear to be sufficient, either alone or in combination with repeat I. In conclusion, no single repeat of α_{1C} seems to be sufficient for depolarization-induced potentiation, which may instead represent a more global property. Several combinations of multiple repeats are

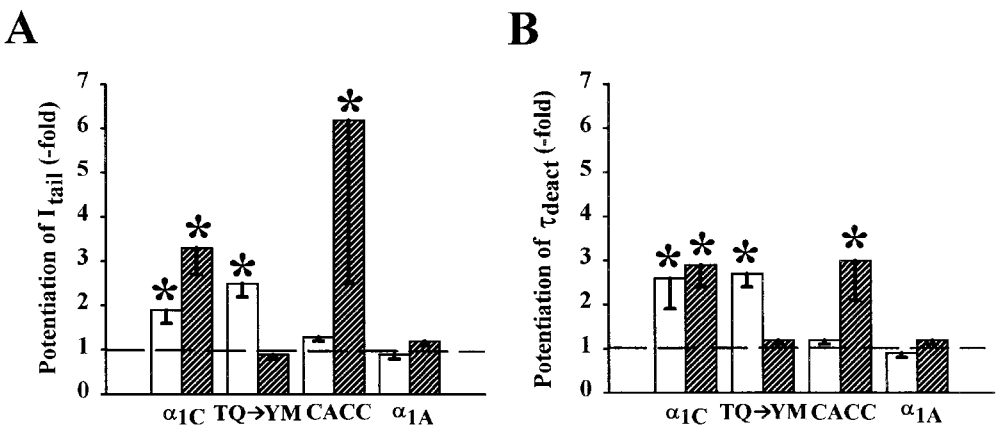

FIGURE 6. Agonist- and depolarization-induced potentiation occur via distinct mechanisms. (A) Average potentiation of tail-current amplitude by strong depolarization ($I_{tail}^{+90}/I_{tail}^{+40}$, white bars) or 10 μM Bay K 8644 ($I_{tail}^{Bay\ K}/I_{tail}^{control}$, hatched bars) for the indicated constructs expressed in dysgenic myotubes. (B) Average potentiation of τ_{deact} by strong depolarization ($\tau_{deact}^{+90}/\tau_{deact}^{+40}$, white bars) or 10 μM Bay K 8644 ($\tau_{deact}^{Bay\ K}/\tau_{deact}^{control}$, hatched bars) for the indicated constructs expressed in dysgenic myotubes. The dashed lines at onefold indicate no potentiation. Asterisks indicate a significant difference ($P < 0.05$) from 1. The number of cells tested in each group ranged from five to eight.

tested by the chimeras examined in this paper, and others cannot be tested because not all possible combinations of repeats of L-type and non–L-type sequence produce functional channels (Grabner et al., 1996; Spaetgens and Zamponi, 1999).

Because potentiation is defined by a shift into a gating mode of substantially increased P_o, it seems likely that potentiation could not occur in a channel already having a relatively high P_o. Therefore, it is of interest to know whether the lack of depolarization-induced potentiation in GFP-CACC and GFP-CCAA is a consequence of an already high P_o. We used Eq. 2 (MATERIALS AND METHODS) to estimate P_o for GFP-α_{1C}, GFP-CACC, GFP-CCAA, and GFP-α_{1A} from measured values of G_{max} and Q_{max}. The values estimated by this approach for both GFP-α_{1C} and GFP-α_{1A} (Table II) are in reasonable agreement with values determined from single-channel measurements for α_{1C} (<0.05; Cachelin et al., 1983; Lew et al., 1991) or α_{1A} (0.6; Llinas et al., 1989). Moreover, as shown in Fig. 7 C, the estimated P_o for GFP-α_{1A} was about 30-fold higher than for GFP-α_{1C}. The estimated P_o for GFP-CCAA was similar to that of GFP-α_{1A}, but estimated P_o for GFP-CACC was much closer to that of GFP-α_{1C} (Fig. 7 C and Table II). The absence of depolarization-induced potentiation for GFP-CACC indicates that a low P_o alone is not a sufficient condition for this process to occur. The lack of depolarization-induced potentiation for GFP-CACC is even more striking given that this construct can be strongly potentiated by agonist.

DISCUSSION

In the present study, we have examined DHP- and depolarization-induced potentiation of L-type Ca^{2+} channels by expressing GFP-tagged cardiac (α_{1C}) and neuronal (α_{1A}) α_1 subunits in dysgenic myotubes. For GFP-α_{1C}, both strong depolarization and agonist (10 μM Bay K 8644) caused tail currents to become larger and to decay more slowly, whereas tail currents for GFP-α_{1A} were not affected by either manipulation. Introduction of two point mutations (T1066Y and Q1070M) into GFP-α_{1C} abolished potentiation by agonist without any evident effect on potentiation by depolarization. Conversely, agonist but not depolarization caused potentiation of a chimera of α_{1C} and α_{1A} (GFP-CACC). Because depolarization-induced potentiation was absent for both GFP-CACC and the chimera GFP-CCAA, it appears that no single repeat of α_{1C} can be responsible for this process. GFP-CACC displayed a relatively low estimated P_o, quite similar to that of GFP-α_{1C}, whereas the estimated P_o for both GFP-CCAA and GFP-α_{1A} was much higher. Therefore, a channel that displays a low P_o (and is potentiated by agonist) can fail to be potentiated by depolarization.

Independent Pathways for Potentiation by DHP Agonist and Depolarization

Unitary records of L-type Ca^{2+} channels have been described as having three modes of gating upon depolarization: mode 0 (null sweeps); mode 1 characterized by brief openings (<1 ms) in bursts; and mode 2 defined by longer openings and high P_o (Hess et al., 1984). Mode 1 is the predominant mode accessed during moderate depolarizations from the holding potential in the absence of DHP agonist, whereas mode 2 is promoted by the presence of agonist (Hess et al., 1984). Strong depolarization also promotes long openings of L-type channels in both chromaffin (Hoshi and Smith, 1987) and cardiac cells (Pietrobon and Hess, 1990). Because we have found that potentiation by either agonist or depolarization can be eliminated without a quantitative reduction in the effect of the other, it appears that these two processes occur via distinct pathways. In addition, we have used a concentration of agonist (10 μM Bay K 8644) that is supramaximal (Kokubun and Reu-

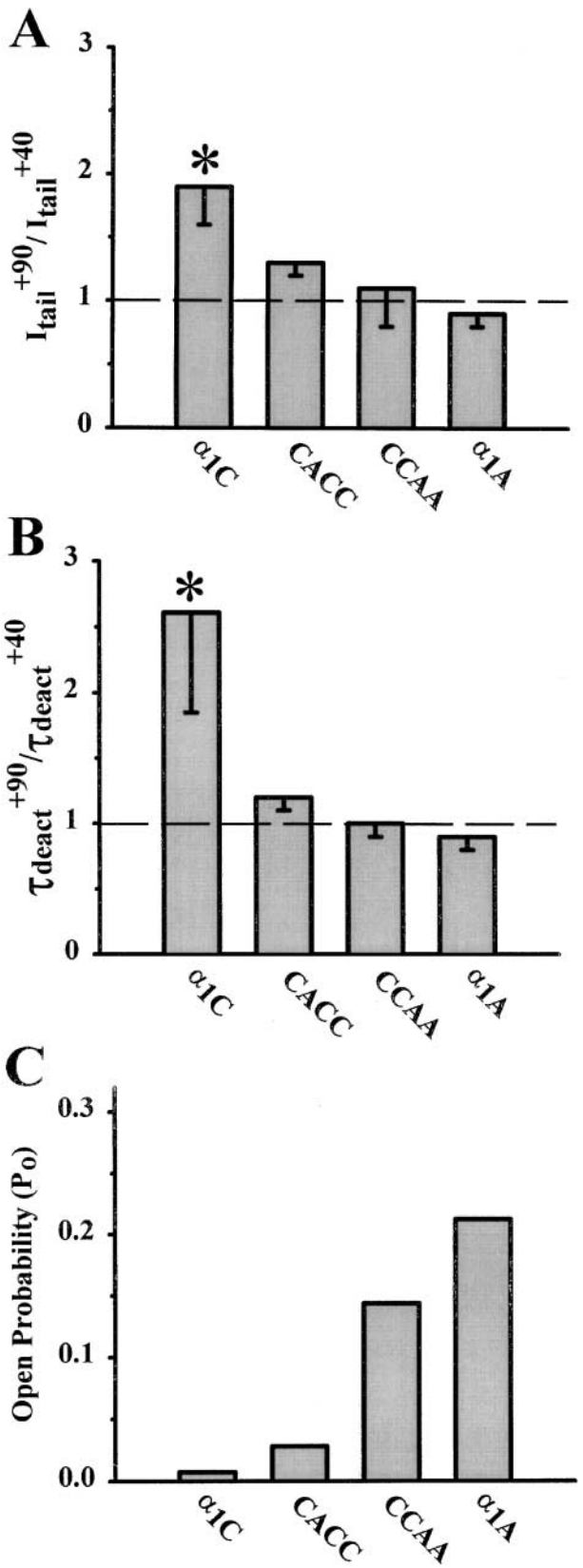

FIGURE 7. Depolarization-induced potentiation cannot be localized to any single channel repeat. Average depolarization-induced potentiation of tail-current amplitude (A), or tail-current deactivation (B) for the indicated constructs. Channel open probability (P_o) for the same constructs (C) was estimated according to Eq. 2 (as described in MATERIALS AND METHODS). Values for P_o were as follows: α_{1C} = 0.01, CACC = 0.03, CCAA = 0.14, and α_{1A} = 0.21. The dashed lines at onefold indicate no potentiation. The number of cells tested in each group ranged from five to eight. Asterisks indicate a significant difference ($P < 0.05$) from 1.

TABLE II

Properties of Wild-type and Chimeric Channels Expressed in Dysgenic Myotubes

	Units	GFP-α_{1C}	GFP-CACC	GFP-CCAA	GFP-α_{1A}
I_{max}	pA/pF	35.2 ± 4.1 (19)	7.0 ± 1.1 (16)	4.8 ± 1.1 (18)	22.3 ± 4.8 (16)
$V_{1/2}$	mV	+6.0 ± 0.6 (10)	+7.6 ± 2.2 (16)	+15.3 ± 1.5 (17)	+18.1 ± 1.7 (12)
G_{max}	nS/nF	436.4 ± 76.1 (13)	118.5 ± 13.8 (16)	105.0 ± 20.7 (18)	352.0 ± 61.9 (16)
Q_{max}	nC/μF	20.9 ± 2.7 (6)	3.0 ± 0.5 (11)	2.9 ± 0.4 (10)	3.2 ± 0.3 (7)
P_o		0.007 (5)	0.028 (6)	0.144 (6)	0.212 (7)

I_{max} is the peak inward current determined by measuring Ca^{2+} currents elicited with 200-ms test depolarizations ranging from −40 to +100 mV. Values for half-maximal activation potential ($V_{1/2}$) and maximal conductance (G_{max}) were determined by fitting peak Ca^{2+} currents according to Eq. 1. Maximum immobilization-resistant charge movement (Q_{max}) was measured by integration of the "On" gating current for a 15-ms step to +40 mV. Open channel probability (P_o) was estimated using Eq. 2 and measured values of $\overline{G_{max}}$ and $\overline{Q_{max}}$ (as described in MATERIALS AND METHODS). All data are presented as mean ± SEM, with numbers in parentheses indicating the number of cells tested.

ter, 1984); therefore, the additional potentiation of tail currents by depolarization in the presence of the agonist also strongly suggests the presence of two independent pathways leading to a potentiated open state. Several other labs have likewise concluded from the additivity of the effects of depolarization and agonist, that these two stimuli cause an increased P_o by distinct pathways (Bourinet et al., 1994; Parri and Lansman, 1996). Moreover, single-channel measurements show both different open times and first latencies depending on whether potentiation is induced by depolarization or agonist (Hoshi and Smith, 1987). In combination, these data suggest not only that mode 2 gating can be accessed by multiple pathways, but also that mode 2 consists of more than one potentiated open state.

Bay K 8644 is well-known to shift activation in the hyperpolarizing direction (Fig. 2; Hess et al., 1984; Sanguinetti et al., 1986), indicating that it shifts equilibrium towards the open state of the channel. We have shown here that mutation of residues T1066 and Q1070 in the IIIS5 transmembrane domain of α_{1C} not only ablates the response to agonist, but also shifts the voltage dependence of activation oppositely, in the depolarizing direction. On this basis, one could hypothesize that Bay K 8644 promotes a conformation of these two resi-

dues that stabilizes open states of the channel, and mutation of these residues destabilizes this conformation.

Role of Accessory Subunits and of Phosphorylation in Depolarization-induced Potentiation

The accessory β subunit has been shown to influence modal gating of α_{1C}. In particular, comparison of α_{1C} expressed with or without the β_{2a} subunit showed that β_{2a} increased both open times and the proportion of long openings (Costantin et al., 1998). β subunits also have been reported to affect depolarization-induced facilitation, which may be mechanistically related to depolarization-induced potentiation (INTRODUCTION). Specifically, depolarization-induced facilitation was found to occur when α_{1C} was coexpressed with the β_1, β_3, or β_4 subunits (Bourinet et al., 1994; Cens et al., 1998), but not with β_{2a} (Cens et al., 1996), raising the possibility that the β subunit plays a direct role in depolarization-induced facilitation of α_{1C}, and perhaps in potentiation as well. However, others have found that depolarization-induced potentiation of the smooth muscle α_{1C} occurs in the absence of any β subunit (Kleppisch et al., 1994). Whatever the exact role of the β subunit, our results demonstrate that depolarization-induced potentiation is strongly influenced by the α_1 subunit itself, because all of the α_1 constructs examined in this study have a conserved "alpha interaction domain" (site of β subunit binding; Pragnell et al., 1994) and were expressed with a common β subunit (β_{1a}, which is endogenous to skeletal muscle; Ruth et al., 1989).

Evidence has been presented that PKA-dependent phosphorylation occurring during depolarizing prepulses is necessary for depolarization-induced facilitation of α_{1S} (Sculptoreanu et al., 1993b; Johnson et al., 1994), the cardiac α_{1C} (Sculptoreanu et al., 1993a), and the neuronal α_{1C} (Sculptoreanu et al., 1995). Evidence also has been presented that phosphorylation during depolarization is not involved in depolarization-induced facilitation of the neuronal α_{1C}, although basal phosphorylation may be required (Bourinet et al., 1994). If phosphorylation is required (either basal or voltage-dependent), then it seems unlikely to involve phosphorylation of α_{1C} directly because truncation of the consensus PKA sites (Gao et al., 1997) of the α_{1C} carboxyl tail does not eliminate depolarization-induced facilitation (Cens et al., 1998). Consistent with this result, we found that depolarization-induced potentiation does not occur for GFP-CACC even though it contains all the consensus PKA sites of α_{1C}.

Structural Determinants of Depolarization-induced Potentiation and Low P_o

As discussed above, brief openings predominate during activation of α_{1C} by modest depolarizations applied from a negative holding potential (mode 1 gating). The conformational changes responsible for activation of these brief openings occur rapidly (macroscopic activation occurs with a time constant of several ms at +30 mV; Tanabe et al., 1991). Depolarization-induced entry into mode 2 occurs on a significantly slower time scale (with a time constant of several hundred ms at +30 mV) and over a much more positive voltage range (Pietrobon and Hess, 1990). Despite these differences, depolarization-induced potentiation resembles mode 1 activation in being strongly voltage-dependent: based on two-state Boltzmann fits, the effective gating charge is 2.5 for depolarization-induced potentiation and 3.2 for mode 1 activation (Pietrobon and Hess, 1990). Thus, the question arises as to the identity of the voltage sensor for depolarization-induced potentiation. One possibility is that, after undergoing the relatively rapid movements leading to mode 1 openings, the S4 segments can undergo subsequent, slower movements in response to still stronger depolarization. It is equally possible that structures other than S4 serve as voltage sensors for depolarization-induced potentiation. Because we found that neither GFP-CACC nor GFP-CCAA undergo depolarization-induced potentiation, it seems unlikely that the voltage-sensing structures for depolarization-induced potentiation are localized within a single repeat. Rather, depolarization-induced potentiation of α_{1C} appears to require large movements of charge distributed throughout the protein.

L-type channels like α_{1S} and α_{1C} differ from α_{1A} channels in that the L-type channels display agonist- and depolarization-induced potentiation, and also have a much lower P_o, raising the possibility that the structural determinants of potentiation and low P_o reside in similar structures. However, the chimera GFP-CACC had a relatively low P_o, yet did not display significant depolarization-induced potentiation. Because the chimera GFP-CCAA displayed a high P_o, the amino-terminal half of α_{1C} (repeats I and II) does not appear to be an important determinant of low P_o; instead, structural requirements for low P_o may reside in the carboxyl half of the protein. Certainly, it is attractive to hypothesize that repeats III and IV are important for the intrinsic, low P_o of L-type channels since these same two repeats play an essential role in agonist binding, which increases P_o. A role for the carboxyl tail in determining P_o is suggested by previous work showing that P_o of α_{1C} is markedly increased by partial truncation of the carboxyl tail (Wei et al., 1994).

As stated earlier, the P_o of the L-type channels containing α_{1C} (<0.05; Cachelin et al., 1983; Lew et al., 1991) is much lower than that of the neuronal channels containing α_{1A} (0.6; Llinas et al., 1989) or α_{1B} (0.5; Delcour and Tsien, 1993). Because single-channel conductance varies less than twofold amongst these channels ([α_{1C}] Kokobun and Reuter, 1984; [α_{1A}] Zhang et al., 1993; [α_{1B}] Rittenhouse and Hess, 1994), the produc-

tion of an equivalent macroscopic current would require a much higher density of the L-type channels. A primary role of L-type Ca^{2+} channels in muscle is to regulate Ca^{2+} movements through ryanodine receptors. For this control to be relatively tight, it may be useful to have an ~1:1 correspondence between the plasmalemmal L-type channels and the intracellular ryanodine receptors. Perhaps this correspondence is best served by a relatively high density of low P_o channels. Conversely, a high P_o and relatively low channel density would be advantageous when it is critical that a cellular response be triggered by the activation of only a few channels. Important goals for future work will be to better define the structures determining the differences in P_o between α_{1C} and neuronal channels like α_{1A} and α_{1B}, and to identify the conformational rearrangements that occur during potentiation of L-type channels.

We thank Kathy Parsons and Lindsay Grimes for performing the tissue culture.

This work was supported by the National Institutes of Health grant NS24444 to K.G. Beam, an NIH predoctoral fellowship MH12512 to C.M. Wilkens, and by the Fonds zur Förderung der Wissenschaftlichen Forschung, Austria (J01242-GEN) to M. Grabner.

Submitted: 26 June 2001
Revised: 24 September 2001
Accepted: 26 September 2001

REFERENCES

Adams, B.A., and K.G. Beam. 1989. A novel Ca^{2+} current in dysgenic skeletal muscle. *J. Gen. Physiol.* 94:429–444.

Adams, B.A., T. Tanabe, A. Mikami, S. Numa, and K.G. Beam. 1990. Intramembrane charge movement restored in dysgenic skeletal muscle by injection of dihydropyridine receptor cDNAs. *Nature.* 346:569–572.

Adams, B.A., Y. Mori, M.S. Kim, T. Tanabe, and K.G. Beam. 1994. Heterologous expression of BI Ca^{2+} channels in dysgenic skeletal muscle. *J. Gen. Physiol.* 104:985–996.

Bourinet, E., P. Charnet, W.J. Tomlinson, A. Stea, T.P. Snutch, and J. Nargeot. 1994. Voltage-dependent facilitation of a neuronal α_{1C} L-type calcium channel. *EMBO J.* 13:5032–5039.

Cachelin, A.B., J.E. de Peyer, S. Kokubun, and H. Reuter. 1983. Ca^{2+} channel modulation by 8-bromocyclic AMP in cultured heart cells. *Nature.* 304:462–464.

Cens, T., M.E. Mangoni, S. Richard, J. Nargeot, and P. Charnet. 1996. Coexpression of the β_2 subunit does not induce voltage-dependent facilitation of the class C L-type Ca^{2+} channel. *Pflügers Arch.* 431:771–774.

Cens, T., S. Restituito, A. Vallentin, and P. Charnet. 1998. Promotion and inhibition of L-type Ca^{2+} channel facilitation by distinct domains of the subunit. *J. Biol. Chem.* 273:18308–18315.

Costantin, J., F. Noceti, N. Qin, X. Wei, L. Birnbaumer, and E. Stefani. 1998. Facilitation by the β_{2a} subunit of pore openings in cardiac Ca^{2+} channels. *J. Physiol.* 507:93–103.

Delcour, A.H., and R.W. Tsien. 1993. Altered prevalence of gating modes in neurotransmitter inhibition of N-type Ca^{2+} channels. *Science.* 259:980–984.

DeMaria, C.D., T.W. Soong, B.A. Alseikhan, R.S. Alvania, and D.T. Yue. 2001. Calmodulin bifurcates the local Ca^{2+} signal that modulates P/Q-type Ca^{2+} channels. *Nature.* 411:484–489.

Gao, T., A. Yatani, M.L. Dell'Acqua, H. Sako, S.A. Green, N. Dascal, J.D. Scott, and M.M. Hosey. 1997. cAMP-dependent regulation of cardiac L-type Ca^{2+} channels requires membrane targeting of PKA and phosphorylation of channel subunits. *Neuron.* 19:185–196.

Gollasch, M., J. Hescheler, J.M. Quayle, J.B. Patlak, and M.T. Nelson. 1992. Single Ca^{2+} channel currents of arterial smooth muscle at physiological Ca^{2+} concentrations. *Am. J. Physiol.* 263: C948–C952.

Grabner, M., Z. Wang, S. Hering, J. Striessnig, and H. Glossmann. 1996. Transfer of 1,4-dihydropyridine sensitivity from L-type to class A (BI) Ca^{2+} channels. *Neuron.* 16:207–218.

Grabner, M., R.T. Dirksen, and K.G. Beam. 1998. Tagging with green fluorescent protein reveals a distinct subcellular distribution of L-type and non-L-type Ca^{2+} channels expressed in dysgenic myotubes. *Proc. Natl. Acad. Sci. USA.* 95:1903–1908.

Hamill, O.P., A. Marty, E. Neher, B. Sakmann, and F.J. Sigworth. 1981. Improved patch-clamp techniques for high-resolution current recording from cells and cell-free membrane patches. *Pflügers Arch.* 391:85–100.

He, M., I. Bodi, G. Mikala, and A. Schwartz. 1997. Motif III S5 of L-type Ca^{2+} channels is involved in the dihydropyridine binding site. A combined radioligand binding and electrophysiological study. *J. Biol. Chem.* 272:2629–2633.

Hess, P., J.B. Lansman, and R.W. Tsien. 1984. Different modes of Ca^{2+} channel gating behaviour favoured by dihydropyridine Ca^{2+} agonists and antagonists. *Nature.* 311:538–544.

Hockerman, G.H., B.D. Johnson, M.R. Abbot, T. Scheuer, and W.A. Catterall. 1997. Molecular determinants of high-affinity phenylalkylamine block of L-type Ca^{2+} channels in transmembrane segment IIIS6 and the pore region of the α_1 subunit. *J. Biol. Chem.* 272:18759–18765.

Horton, R.M., H.D. Hunt, S.N. Ho, J.K. Pullen, and L.R. Pease. 1989. Engineering hybrid genes without the use of restriction enzymes: gene splicing by overlap extension. *Gene.* 77:61–68.

Hoshi, T., and S.J. Smith. 1987. Large depolarization induces long openings of voltage-dependent Ca^{2+} channels in adrenal chromaffin cells. *J. Neurosci.* 7:571–580.

Ito, H., N. Klugbauer, and F. Hofmann. 1997. Transfer of the high affinity dihydropyridine sensitivity from L-type to non-L-type Ca^{2+} channel. *Mol. Pharmacol.* 52:735–740.

Johnson, B.D., T. Scheuer, and W.A. Catterall. 1994. Voltage-dependent potentiation of L-type Ca^{2+} channels in skeletal muscle cells requires anchored cAMP-dependent protein kinase. *Proc. Natl. Acad. Sci. USA.* 91:11492–11496.

Kleppisch, T., K. Pedersen, C. Strubing, E. Bosse-Doenecke, V. Flockerzi, F. Hofmann, and J. Hescheler. 1994. Double-pulse facilitation of smooth muscle α_1 subunit Ca^{2+} channels expressed in CHO cells. *EMBO J.* 13:2502–2507.

Knudson, C.M., N. Chaudhari, A.H. Sharp, J.A. Powell, K.G. Beam, and K.P. Campbell. 1989. Specific absence of the α_1 subunit of the dihydropyridine receptor in mice with muscular dysgenesis. *J. Biol. Chem.* 264:1345–1348.

Kokubun, S., and H. Reuter. 1984. Dihydropyridine derivatives prolong the open state of Ca^{2+} channels in cultured cardiac cells. *Proc. Natl. Acad. Sci. USA.* 81:4824–4827.

Lee, A., T. Scheuer, and W.A. Catterall. 2000. Ca^{2+}/calmodulin-dependent facilitation and inactivation of P/Q-type type Ca^{2+} channels. *J. Neurosci.* 20:6830–6838.

Lew, W.Y., L.V. Hryshko, and D.M. Bers. 1991. Dihydropyridine receptors are primarily functional L-type Ca^{2+} channels in rabbit ventricular myocytes. *Circ. Res.* 69:1139–1145.

Llinas, R.R., M. Sugimori, and B. Cherksey. 1989. Voltage-dependent Ca^{2+} conductances in mammalian neurons. The P channel. *Ann. NY Acad. Sci.* 560:103–111.

Mikami, A., K. Imoto, T. Tanabe, T. Niidome, Y. Mori, H. Takeshima, S. Narumiya, and S. Numa. 1989. Primary structure

and functional expression of the cardiac dihydropyridine-sensitive Ca^{2+} channel. *Nature.* 340:230–233.

Mitterdorfer, J., Z. Wang, M.J. Sinnegger, S. Hering, J. Striessnig, M. Grabner, and H. Glossmann. 1996. Two amino acid residues in the IIIS5 segment of L-type Ca^{2+} channels differentially contribute to 1,4-dihydropyridine sensitivity. *J. Biol. Chem.* 271:30330–30335.

Mori, Y., T. Friedrich, M.S. Kim, A. Mikami, J. Nakai, P. Ruth, E. Bosse, F. Hofmann, V. Flockerzi, et al. 1991. Primary structure and functional expression from complementary DNA of a brain Ca^{2+} channel. *Nature.* 350:398–402.

Noceti, F., P. Baldelli, X. Wei, N. Qin, L. Toro, L. Birnbaumer, and E. Stefani. 1996. Effective gating charges per channel in voltage-dependent K^+ and Ca^{2+} channels. *J. Gen. Physiol.* 108:143–155.

Nowycky, M.C., A.P. Fox, and R.W. Tsien. 1985. Long-opening mode of gating of neuronal Ca^{2+} channels and its promotion by the dihydropyridine Ca^{2+} agonist Bay K 8644. *Proc. Natl. Acad. Sci. USA.* 82:2178–2182.

Parri, H.R., and J.B. Lansman. 1996. Multiple components of Ca^{2+} channel facilitation in cerebellar granule cells: expression of facilitation during development in culture. *J. Neurosci.* 16:4890–4902.

Pietrobon, D., and P. Hess. 1990. Novel mechanism of voltage-dependent gating in L-type Ca^{2+} channels. *Nature.* 346:651–655.

Pragnell, M., M. De Waard, Y. Mori, T. Tanabe, T.P. Snutch, and K.P. Campbell. 1994. Ca^{2+} channel β subunit binds to a conserved motif in the I-II cytoplasmic linker of the α_1 subunit. *Nature.* 368: 67–70.

Reuter, H. 1983. Ca^{2+} channel modulation by neurotransmitters, enzymes and drugs. *Nature.* 301:569–574.

Rittenhouse, A.R., and P. Hess. 1994. Microscopic heterogeneity in unitary N-type Ca^{2+} currents in rat sympathetic neurons. *J. Physiol.* 474:87–99.

Ruth, P., A. Rohrkasten, M. Biel, E. Bosse, S. Regulla, H.E. Meyer, V. Flockerzi, and F. Hofmann. 1989. Primary structure of the β subunit of the DHP-sensitive Ca^{2+} channel from skeletal muscle. *Science.* 245:1115–1118.

Sanguinetti, M.C., D.S. Krafte, and R.S. Kass. 1986. Voltage-dependent modulation of Ca^{2+} channel current in heart cells by Bay K8644. *J. Gen. Physiol.* 88:369–392.

Sather, W.A., T. Tanabe, J.F. Zhang, Y. Mori, M.E. Adams, and R.W. Tsien. 1993. Distinctive biophysical and pharmacological properties of class A (BI) Ca^{2+} channel α_1 subunits. *Neuron.* 11:291–303.

Sculptoreanu, A., E. Rotman, M. Takahashi, T. Scheuer, and W.A. Catterall. 1993a. Voltage-dependent potentiation of the activity of cardiac L-type Ca^{2+} channel α_1 subunits due to phosphorylation by cAMP-dependent protein kinase. *Proc. Natl. Acad. Sci. USA.* 90:10135–10139.

Sculptoreanu, A., T. Scheuer, and W.A. Catterall. 1993b. Voltage-dependent potentiation of L-type Ca^{2+} channels due to phosphorylation by cAMP-dependent protein kinase. *Nature.* 364:240–243.

Sculptoreanu, A., A. Figourov, and W.C. De Groat. 1995. Voltage-dependent potentiation of neuronal L-type Ca^{2+} channels due to state-dependent phosphorylation. *Am. J. Physiol.* 269:C725–C732.

Sinnegger, M.J., Z. Wang, M. Grabner, S. Hering, J. Striessnig, H. Glossmann, and J. Mitterdorfer. 1997. Nine L-type amino acids confer full 1,4-dihydropyridine sensitivity to the neuronal Ca^{2+} channel α_{1A} subunit: role of L-type Met-1188. *J. Biol. Chem.* 272: 27686–27693.

Spaetgens, R.L., and G.W. Zamponi. 1999. Multiple structural domains contribute to voltage-dependent inactivation of rat brain α_{1E} Ca^{2+}channels. *J. Biol. Chem.* 274:22428–22436.

Tanabe, T., B.A. Adams, S. Numa, and K.G. Beam. 1991. Repeat I of the dihydropyridine receptor is critical in determining Ca^{2+} channel activation kinetics. *Nature.* 352:800–803.

Tanabe, T., A. Mikami, T. Niidome, S. Numa, B.A. Adams, and K.G. Beam. 1993. Structure and function of voltage-dependent Ca^{2+} channels from muscle. *Ann. NY Acad. Sci.* 707:81–86.

Tsien, R.W., D. Lipscombe, D.V. Madison, K.R. Bley, and A.P. Fox. 1988. Multiple types of neuronal Ca^{2+} channels and their selective modulation. *Trends Neurosci.* 11:431–438.

Wei, X., A. Neely, A.E. Lacerda, R. Olcese, E. Stefani, E. Perez-Reyes, and L. Birnbaumer. 1994. Modification of Ca^{2+}channel activity by deletions at the carboxyl terminus of the cardiac α_1 subunit. *J. Biol. Chem.* 269:1635–1640.

Zhang, J.F., A.D. Randall, P.T. Ellinor, W.A. Horne, W.A. Sather, T. Tanabe, T.L. Schwarz, and R.W. Tsien. 1993. Distinctive pharmacology and kinetics of cloned neuronal Ca^{2+} channels and their possible counterparts in mammalian CNS neurons. *Neuropharmacology.* 32:1075–1088.

Zühlke, R.D., G.S. Pitt, R.W. Tsien, and H. Reuter. 2000. Ca^{2+}-sensitive inactivation and facilitation of L-type Ca^{2+} channels both depend on specific amino acid residues in a consensus calmodulin-binding motif in the α_{1C} subunit. *J. Biol. Chem.* 275:21121–21129.